

Polarization Cross Sections in Proton Compton Scattering*

GARY K. GREENHUT

Physics Department, Northeastern University, Boston, Massachusetts 02115

(Received 13 October 1969)

A phenomenological amplitude for proton Compton scattering is obtained, and fits are made to the differential cross-section data. The amplitude is used to calculate the cross sections for the Compton scattering of polarized photons and the polarization of the recoil proton. It is found that the polarized-photon cross sections are sensitive to the amount of P_{11} resonance in the scattering amplitude.

I. INTRODUCTION

OVER the past few years, there have been a number of experiments probing the electromagnetic interactions of the proton through proton Compton scattering. Until recently, the data have been restricted to measurements of cross sections,^{1,2} and as yet there have been no experiments on recoil-nucleon polarization. There has, however, been a recent experiment on proton Compton scattering using polarized photons.³

In this paper, we compare the results of the polarized-photon Compton scattering experiment with the predictions of a phenomenological amplitude for Compton scattering originally introduced in a calculation of the two-photon-exchange effect in electron-proton scattering.⁴ In Sec. II, we introduce the Compton scattering amplitude and, in Sec. III, calculate the polarized-photon Compton scattering cross sections. Defining $d\sigma_{11}/d\Omega$ ($d\sigma_{\perp}/d\Omega$) to be the differential cross section for the incoming photon polarized parallel (perpendicular) to the reaction plane, it is found that $d\sigma_{11}/d\sigma_{\perp}$ is quite sensitive to the amount of P_{11} resonance in the scattering amplitude. In Sec. IV a calculation is made of the recoil-proton polarization, and in Sec. V the validity of the amplitude used in these calculations is discussed.

II. PROTON COMPTON SCATTERING AMPLITUDE

The early theoretical treatment of proton Compton scattering involved the use of dispersion relations and the Mandelstam representation of the scattering amplitudes.⁵ Quantitative calculations of nucleon Compton scattering cross sections have been done for incident laboratory photon energies up to 400 MeV,

* Work supported in part by the National Science Foundation, under Grant No. GP-9217.

¹ D. R. Rust *et al.*, Phys. Rev. Letters **15**, 938 (1965) (center-of-mass scattering angle of 90°); M. Deutsch *et al.*, in *Proceedings of the 1967 International Symposium on Electron and Photon Interactions at High Energies* (Clearinghouse for Federal Scientific and Technical Information, Springfield, Va., 1968), p. 619 (center-of-mass scattering angle of 65°).

² P. S. Baranov *et al.*, Yadern. Fiz. **3**, 1083 (1966) [English transl.: Soviet J. Nucl. Phys. **3**, 791 (1966)] (angular distributions at 210 and 245 MeV); E. R. Gray and A. O. Hanson, Phys. Rev. **160**, 1212 (1967) (angular distribution at 310 MeV).

³ G. Barbiellini *et al.*, Phys. Rev. **174**, 1665 (1968).

⁴ G. K. Greenhut, Phys. Rev. **184**, 1860 (1969).

⁵ M. Gell-Mann, M. L. Goldberger, and W. E. Thirring, Phys. Rev. **95**, 1612 (1954); A. C. Hearn and E. Leader, *ibid.* **126**, 789 (1962); A. P. Contogouris, Nuovo Cimento **25**, 104 (1962).

i.e., through the first proton resonance.⁶ Up to this energy, the unitarity sum must include the nucleon pole terms and the π - N intermediate states in the s channel and the π^0 and η^0 pole terms and the π - π intermediate states in the t channel. Above this energy, the number of intermediate states that must be included in the unitarity sum increases rapidly, greatly limiting the usefulness of this approach.

Some time ago, a model was introduced⁷ for the purpose of treating proton Compton scattering up to incident laboratory photon energies of the order of 1 GeV. The model approximates the dispersion integrals by replacing them with Breit-Wigner resonance terms corresponding to the major nucleon resonances. We shall use this model in an extended form, introducing the proton Born terms with the correct low-energy limit,⁸ π^0 and η^0 pole terms, and crossing-symmetric Breit-Wigner resonance terms. Each resonance term has one free parameter which is varied to fit the proton Compton scattering cross-section data.

The S matrix for Compton scattering in the center-of-mass system is given by

$$S = ie^2(2\pi)^4 \delta^4(k + P_i - k' - P_f) (M/\omega \mathcal{E}) T_C,$$

where k and k' are the initial and final photon momenta with energy component ω , and P_i and P_f are the initial and final proton momenta with energy component \mathcal{E} . In the center-of-mass frame,

$$\begin{aligned} T_C = & R_1(\mathbf{e} \cdot \mathbf{e}') + (R_2/\omega^2)[(\mathbf{k} \times \mathbf{e}) \cdot (\mathbf{k}' \times \mathbf{e}')] \\ & + iR_3[\boldsymbol{\sigma} \cdot (\mathbf{e}' \times \mathbf{e})] \\ & + i(R_4/\omega^2)\{\boldsymbol{\sigma} \cdot [(\mathbf{k}' \times \mathbf{e}') \times (\mathbf{k} \times \mathbf{e})]\} \\ & + i(R_5/\omega^2)\{(\boldsymbol{\sigma} \cdot \mathbf{k})[\mathbf{k}' \cdot (\mathbf{e}' \times \mathbf{e})] \\ & \quad - (\boldsymbol{\sigma} \cdot \mathbf{k}')[\mathbf{k} \cdot (\mathbf{e} \times \mathbf{e}')] \} \\ & + i(R_6/\omega^2)\{(\boldsymbol{\sigma} \cdot \mathbf{k}')[\mathbf{k}' \cdot (\mathbf{e}' \times \mathbf{e})] \\ & \quad - (\boldsymbol{\sigma} \cdot \mathbf{k})[\mathbf{k} \cdot (\mathbf{e} \times \mathbf{e}')] \}. \end{aligned} \quad (2.1)$$

The six scalar functions in (2.1) are decomposed as follows:

$$R_i = R_i^B + R_i^L + R_i^r,$$

where R_i^B is the proton Born-term contribution, R_i^L is the combined contribution of the π^0 and η^0 pole terms,

⁶ R. Koberle, Phys. Rev. **166**, 1558 (1968).

⁷ Y. Nagashima, Progr. Theoret. Phys. (Kyoto) **33**, 828 (1965).

⁸ M. Gell-Mann and M. L. Goldberger, Phys. Rev. **96**, 1433 (1954); F. E. Low, *ibid.* **96**, 1428 (1954).

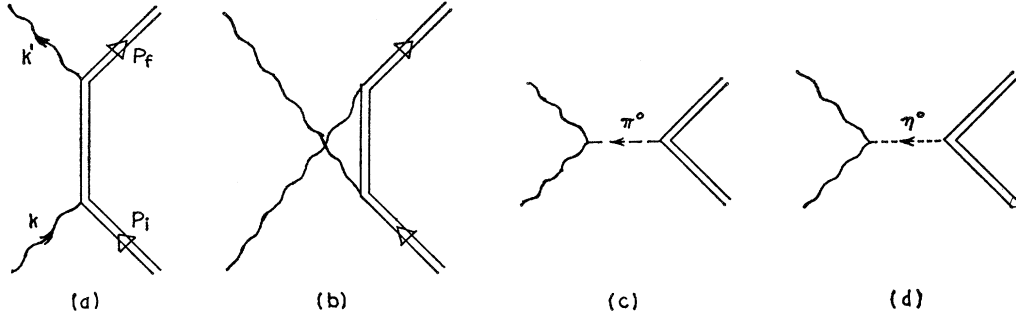


FIG. 1. One-particle intermediate states in proton Compton scattering: (a) and (b) Born terms; (c) π^0 pole term; (d) η^0 pole term.

and R_i^B is the combined contribution of the proton s -channel resonance terms. The diagrams corresponding to the Born and pole terms are shown in Fig. 1.

The contributions to the scattering amplitude from the diagrams in Figs. 1(a) and 1(b) require some discussion. When treating proton Compton scattering in dispersion theory, the contributions are obtained by calculating the one-proton intermediate-state term in the s -channel unitarity sum using the usual proton current

$$J_\mu = u(P_f) [\gamma_\mu F_1(q^2) + (i\sigma_{\mu\nu} q^\nu / 2M) \kappa F_2(q^2)] u(P_i), \quad (2.2)$$

where q is the four-momentum transfer, M is the mass of the proton, and κ is its anomalous magnetic moment. The results of this calculation are known not to obey the low-energy theorems,⁸ and normally subtractions are introduced in the dispersion relations in order to obtain the correct low-energy behavior.⁹ In order to insure correct low-energy behavior, we shall use amplitudes obtained directly from the diagrams in Figs. 1(a) and 1(b) using the proton current (2.2) and Feynman rules. These amplitudes are known to have the correct low-energy behavior to lowest order in the photon frequency.⁸

The proton Born-term contributions are given by⁵

$$R_1^B = -\frac{\mathcal{E} + M - (\mathcal{E} - M)x}{2M(1-x^2)} (A_3 + xA_1) - \frac{(\mathcal{E} + M)(V - M) + (\mathcal{E} - M)(V + M)x}{4M^2(1-x^2)} (A_4 + xA_2),$$

TABLE I. Parameters for the π^0 and η^0 amplitudes.

	$g^2/4\pi$	m (MeV)	τ (sec)
π^0	14	135	0.89×10^{-16}
η^0	8	549	0.54×10^{-18}

⁹ However, see H. Pagels, Phys. Rev. **158**, 1566 (1967), where the low-energy theorems, combined with a no-subtraction hypothesis supported by Regge-pole asymptotic behavior, are used to derive sum rules for the lifetimes of the π^0 and η^0 .

$$R_2^B = -R_1^B \quad (\text{with } A_3 \leftrightarrow A_1, A_4 \leftrightarrow A_2),$$

$$R_3^B = -\frac{\mathcal{E} - M}{2M} \left(A_1 - \frac{V + M}{2M} A_2 \right),$$

$$R_4^B = -R_3^B \quad (\text{with } A_1 \rightarrow A_3, A_2 \rightarrow A_4),$$

$$R_5^B = \frac{\mathcal{E} - M}{2M(1-x^2)}$$

$$\times \left[-A_3 + \frac{V + M}{2M} A_4 - \left(A_1 - \frac{V + M}{2M} A_2 \right) x \right] - \frac{\omega V}{8M^2(1+x)} A_5 + \frac{\omega}{4M(1-x)} A_6,$$

$$R_6^B = -R_5^B \quad (\text{with } A_3 \leftrightarrow A_1, A_4 \leftrightarrow A_2, A_6 \rightarrow -A_6),$$

where $x = \cos\theta^*$, θ^* being the c.m. scattering angle, and V is the total c.m. energy

$$V = \omega + (M^2 + \omega^2)^{1/2} = \omega + \mathcal{E}.$$

The functions A_i are

$$A_1 = -2M \left(\frac{1}{M^2 - s} + \frac{1}{M^2 - u} \right),$$

$$A_2 = -2M \left(\frac{1}{M^2 - s} - \frac{1}{M^2 - u} \right),$$

$$A_3 = -\frac{1 - (1 + \kappa)^2}{M},$$

$$A_4 = 2M(1 + \kappa)^2 \left(\frac{1}{M^2 - s} - \frac{1}{M^2 - u} \right),$$

$$A_5 = -4M(1 + \kappa) \left(\frac{1}{M^2 - s} + \frac{1}{M^2 - u} \right) - \frac{2\kappa^2}{M},$$

$$A_6 = 2M(1 + \kappa) \left(\frac{1}{M^2 - s} + \frac{1}{M^2 - u} \right) + \frac{(1 + \kappa)^2 - 1}{M},$$

$$s = V^2, \quad t = -2\omega^2(1 - x), \quad u = 2M^2 - V^2 + 2\omega^2(1 - x).$$

TABLE II. Parameters associated with the proton resonances.

i	Resonance	M_i^* (MeV)	Γ_{0i} (MeV)	$L_{2I, 2J^P}$	Dominant partial-wave amplitude	ω_i (MeV)	ω_i^{lab} (MeV)	h_i (MeV)
1	$\Delta(1236)$	1236	120	P_{33}^+	f_{MM}^{1+}	262	346	231
2	$N(1400)$	1400	200	P_{11}^+	f_{MM}^{1-}	386	578	367
3	$N(1525)$	1525	105	D_{13}^-	f_{EE}^{1+}	474	771	460
4	$N(1688)$	1688	110	F_{15}^+	f_{EE}^{2+}	584	1050	573

The π^0 and η^0 pole terms are obtained using the standard π - N coupling at the proton vertex¹⁰ and the following coupling at the photon vertex:

$$-f\epsilon^{\mu\nu\alpha\beta}b_\mu(k+k')_\nu e_\alpha e'_\beta,$$

where e and e' are the polarization four-vectors of the incoming and outgoing photons, b is the momentum carried by the intermediate particle as in Figs. 1(c) and 1(d), and

$$f^2/4\pi = 4/m^2(m\tau).$$

Here m is the mass of the exchanged meson, and τ is its lifetime for decay into two photons. The contribution of π^0 and η^0 exchange to (2.1) can then be written

$$R_1^L = R_2^L = R_3^L = R_4^L = 0,$$

$$R_5^L = -\frac{1}{\alpha M} \left\{ \left(\frac{g_\pi^2}{4\pi} \right)^{1/2} \frac{1}{m_\pi(m_\pi\tau_\pi)^{1/2}} \frac{1}{1-x+m_\pi^2/2\omega^2} + \left(\frac{g_\eta^2}{4\pi} \right)^{1/2} \frac{1}{m_\eta(m_\eta\tau_\eta)^{1/2}} \frac{1}{1-x+m_\eta^2/2\omega^2} \right\}, \quad (2.3)$$

$$R_6^L = -R_5^L.$$

The parameters appearing in (2.3) are given in Table I.¹¹

We next develop a representation of the s -channel proton resonance contributions. The point of view taken here will be that these contributions arise from the π - N intermediate state—for instance, in the s -channel unitarity sum in the dispersion approach. Thus, the resonance representation, which will be a Breit-Wigner

resonance form, is an approximation to the dispersion integral over the product of single-pion photoproduction amplitudes. We will therefore require that the representations have smooth and approximately correct threshold behavior in the pion momentum at the value of the photon energy equal to the threshold for the production of one pion plus a nucleon in the intermediate state. We will also use a criterion for the consideration of a proton resonance based on its elasticity in the π - N channel.

We shall be concerned with proton Compton scattering up to an incident laboratory photon energy of about 1 GeV. Beyond this energy, the data¹ show a rapid decrease with energy, indicating the onset of diffractive behavior. In the energy region of interest, multipion intermediate states do appear, although they will not be taken into account explicitly. Their effect is, in some sense, present in the final amplitude, however, since a purely phenomenological fit is made to the data to obtain the resonance couplings.

The criteria for including a resonance in the amplitude will be that its mass be less than 1700 MeV so that it can appear as an intermediate state for laboratory photons with energies up to 1 GeV, and that its elasticity into the π - N channel be greater than 50%. The four resonances satisfying these criteria are listed in Table II, along with their masses (M_i^*), widths (Γ_{0i}), orbital angular momentum (L), spin (S), parity (P), and isotopic spin (I).

A partial-wave decomposition of the Compton scattering amplitude in the center-of-mass system gives the following results for the scalar functions in (2.1)⁵:

$$R_1 = \sum_{l=1}^{\infty} \{ [(l+1)f_{EE}^{l+} + lf_{EE}^{l-}] (P_l' + xP_l'') - [(l+1)f_{MM}^{l+} + lf_{MM}^{l-}] P_l'' \},$$

$$R_2 = R_1 \quad (\text{with } E \leftrightarrow M),$$

$$R_3 = \sum_{l=1}^{\infty} \{ (f_{EE}^{l+} - f_{EE}^{l-}) (-P_l' - 3xP_l'' + (1-x^2)P_l''') - (f_{MM}^{l+} - f_{MM}^{l-}) P_l'' + f_{EM}^{l-} [(l-1)P_l' - xP_l''] + (f_{ME}^{l-} - f_{ME}^{l+}) P_l'' + f_{EM}^{l+} [(l+2)P_l' + xP_l''] \}, \quad (2.4)$$

$$R_4 = R_3 \quad (\text{with } E \leftrightarrow M),$$

¹⁰ J. D. Bjorken and S. D. Drell, *Relativistic Quantum Mechanics* (McGraw-Hill Book Co., New York, 1964).

¹¹ J. S. Ball, Phys. Rev. **149**, 1191 (1966) (η - p coupling); C. Bemporad *et al.*, Phys. Letters **25B**, 380 (1967) (η lifetime).

$$R_5 = \sum_{l=1}^{\infty} \left\{ (f_{EE^{l+}} - f_{EE^{l-}})(2P_l'' + P_l''') - (f_{MM^{l+}} - f_{MM^{l-}})P_l''' + \frac{1}{2}f_{EM^{l-}}[(l-4)P_l'' - 2xP_l'''] \right. \\ \left. + \frac{1}{2}f_{ME^{l-}}[2(1-l)P_l' + (4-l)xP_l'' + (1+x^2)P_l'''] - \frac{1}{2}f_{ME^{l+}}[2(l+2)P_l' + (l+5)P_l'' \right. \\ \left. + (x^2+1)P_l'''] + \frac{1}{2}f_{EM^{l+}}[(l+5)P_l'' + 2xP_l'''] \right\},$$

$$R_6 = R_5 \quad (\text{with } E \leftrightarrow M),$$

where $P_l^{(n)} \equiv (d/dx)^n P_l(x)$, P_l being the l th-order Legendre polynomial, and $f_{EE^{l\pm}}$ is the partial-wave amplitude for the transition $|j=l\pm\frac{1}{2}, E, l\rangle \rightarrow |j=l\pm\frac{1}{2}, E, l\rangle$, and similarly for $f_{MM^{l\pm}}$, $f_{EM^{l\pm}}$, and $f_{ME^{l\pm}}$. E and M denote an electric and magnetic multipole state, respectively.

It is well known that in single-pion photoproduction the $\Delta(1236)$ contributes mainly in the magnetic dipole partial wave. Analyses of photoproduction¹² show that the electric quadrupole amplitude is of the order of 10% the magnetic dipole amplitude in the region of the resonance. It has been shown¹³ that the inclusion of a small amount of electric quadrupole in the over-all amplitude does not alter the resulting cross section very much but only changes, by a small amount, the details of the angular distribution. In the following, we shall

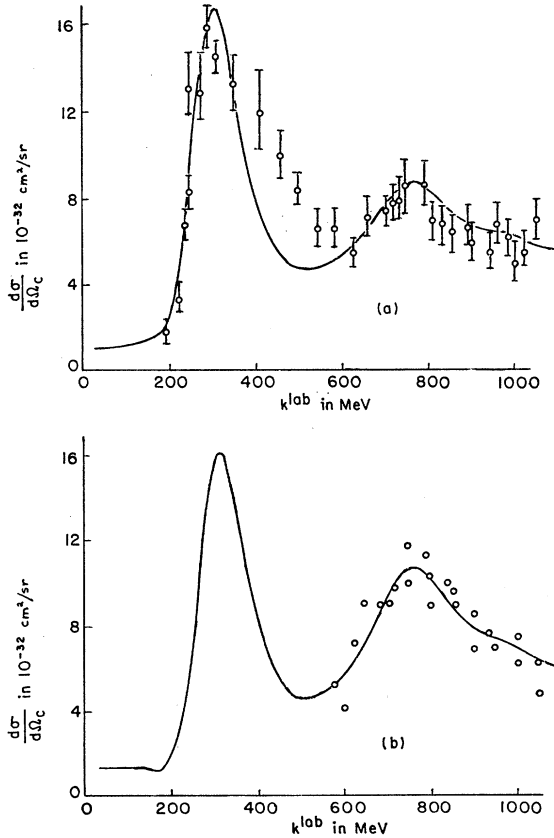


FIG. 2. Fit to the proton Compton scattering data (set *a*): (a) $\theta^* = 90^\circ$; (b) $\theta^* = 65^\circ$.

¹² E.g., the Walker analysis as reported in S. L. Adler and E. J. Gilman, Phys. Rev. 152, 1460 (1966).

¹³ A. P. Contogouris, Phys. Rev. 124, 912 (1961).

consider only the magnetic dipole partial-wave amplitude $f_{MM^{l+}}$ for the $\Delta(1236)$ resonance. In an analogous way, only one partial-wave amplitude will be used for each of the remaining three resonances. These amplitudes are listed in Table III.

The resonance contributions to the scalar amplitudes in (2.1) are decomposed as follows:

$$R_i^r = R_i^{(1)} + R_i^{(2)} + R_i^{(3)} + R_i^{(4)}.$$

Using (2.4), we obtain the following contributions:

for $\Delta(1236)$:

$$R_1^{(1)} = R_3^{(1)} = R_5^{(1)} = R_6^{(1)} = 0, \\ R_2^{(1)} = 2f_{MM^{1+}}, \quad R_4^{(1)} = -\hat{f}_{MM^{1+}}; \quad (2.5a)$$

for $N(1400)$:

$$R_1^{(2)} = R_3^{(2)} = R_5^{(2)} = R_6^{(2)} = 0, \\ R_2^{(2)} = f_{MM^{1-}}, \quad R_4^{(2)} = \hat{f}_{MM^{1-}}; \quad (2.5b)$$

for $N(1525)$:

$$R_1^{(3)} = 2f_{EE^{1+}}, \quad R_3^{(3)} = -\hat{f}_{EE^{1+}}, \\ R_2^{(3)} = R_4^{(3)} = R_5^{(3)} = R_6^{(3)} = 0; \quad (2.5c)$$

for $N(1688)$:

$$R_1^{(4)} = 18f_{EE^{2+}}, \quad R_2^{(4)} = -9f_{EE^{2+}}, \quad R_3^{(4)} = -12\hat{f}_{EE^{2+}}, \\ R_4^{(4)} = -3\hat{f}_{EE^{2+}}, \quad R_5^{(4)} = 6\hat{f}_{EE^{2+}}, \quad R_6^{(4)} = 0. \quad (2.5d)$$

Crossing symmetry at $\theta^* = 180^\circ$ in expression (2.1) gives the following relations:

$$R_1(\omega) - R_2(\omega) = R_1(-\omega) - R_2(-\omega), \\ R_3(\omega) - R_4(\omega) - 2R_5(\omega) + 2R_6(\omega) \\ = -[R_3(-\omega) - R_4(-\omega) - 2R_5(-\omega) + 2R_6(-\omega)].$$

We have distinguished between the amplitudes associated with R_1 and R_2 and with R_3 through R_6 in (2.5), the latter having a caret, because of their different behavior under crossing.

Redefining the partial-wave amplitudes

$$f_1 \equiv f_{MM^{1+}}, \quad f_2 \equiv f_{MM^{1-}}, \quad f_3 \equiv f_{EE^{1+}}, \quad f_4 \equiv f_{EE^{2+}},$$

TABLE III. Fits to the unpolarized-proton Compton scattering data.

Set	C_1 [$\Delta(1236)$]	C_2 [$N(1400)$]	C_3 [$N(1525)$]	C_4 [$N(1688)$]
<i>a</i>	0.46	0.35	0.55	0.10
<i>b</i>	0.46	0.24	0.57	0.12
<i>c</i>	0.46	0.12	0.61	0.14
<i>d</i>	0.46	0	0.65	0.16

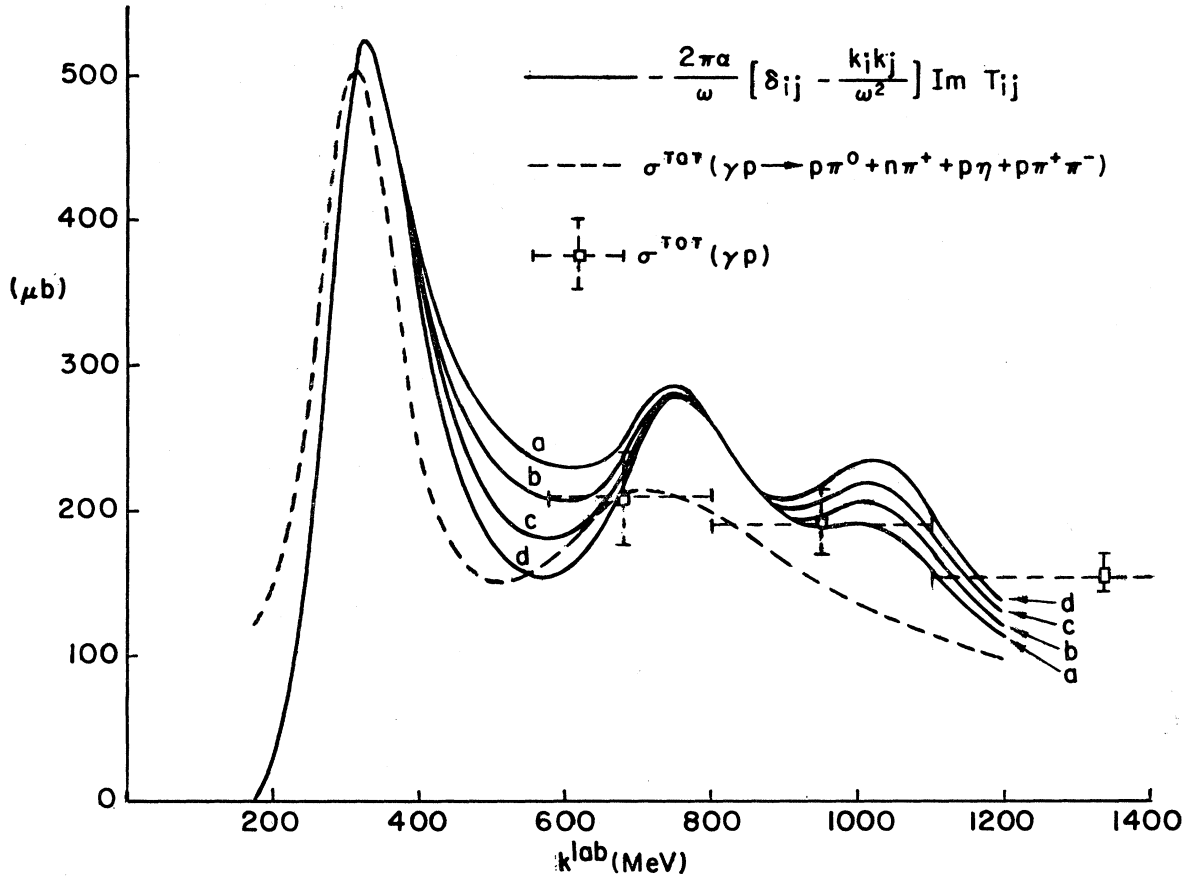


Fig. 3. Comparison of the phenomenological amplitude with total γp cross sections. The letters correspond to the sets of constants in Table III. The dashed line is from Ref. 14; the experimental points are from Ref. 15.

and similarly for the careted amplitudes, the amplitudes are given the following crossing-symmetric Breit-Wigner form,

$$f_i = \frac{C_i}{|\omega|} \frac{1}{2} \Gamma_i \left[\frac{1}{\omega - \omega_i + i \frac{1}{2} \Gamma_i} - \frac{1}{\omega + \omega_i - i \frac{1}{2} \Gamma_i} \right], \quad (2.6)$$

$$\hat{f}_i = \frac{C_i}{|\omega|} \frac{1}{2} \Gamma_i \left[\frac{1}{\omega - \omega_i + i \frac{1}{2} \Gamma_i} + \frac{1}{\omega + \omega_i - i \frac{1}{2} \Gamma_i} \right],$$

where

$$\omega_i = [(M_i^*)^2 - M^2] / 2M_i^*$$

are the c.m. photon resonance energies given in Table II along with the laboratory photon resonance energies

$$\omega_i^{\text{lab}} = (M_i^*/M)\omega_i.$$

The Γ_i are the energy-dependent widths of the proton resonances and the C_i are real coupling constants

determined by a fit to the proton Compton scattering data.

The resonance widths are given by

$$\Gamma_i = \Gamma_{0i} \left| \frac{h}{h_i} \frac{v_L(|hd|)}{v_L(|hd|)} \theta(|\omega| - \omega) \right|, \quad (2.7)$$

where L is the orbital angular momentum of the resonance and

$$v_L^{(Z)} = \frac{1}{j_L^2(Z) + n_L^2(Z)},$$

j_L and n_L being the spherical Bessel and Neumann functions of order L , respectively. The energy ω_T is the threshold photon energy in the c.m. system for single-pion production and is equal to 131 MeV (151 MeV in the laboratory system). The factor h is the c.m. pion momentum

$$h = \frac{\{[V + (M + m_\pi)][V - (M + m_\pi)][V + (M - m_\pi)][V - (M - m_\pi)]\}^{1/2}}{2V} \quad (2.8)$$

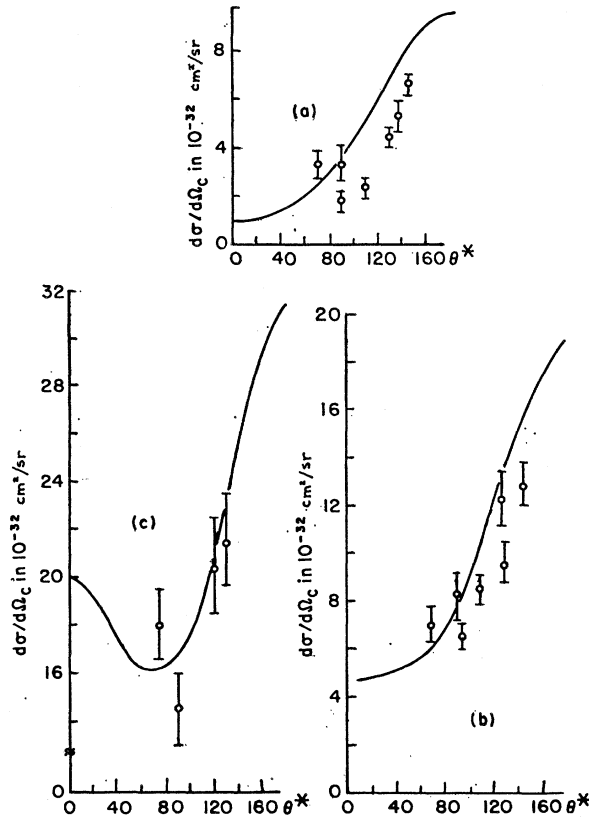


FIG. 4. Comparison of the phenomenological cross section with angular distribution data for proton Compton scattering (set *a*): (a) $\omega^{\text{lab}} = 210$ MeV; (b) $\omega^{\text{lab}} = 245$ MeV; (c) $\omega^{\text{lab}} = 310$ MeV.

and h_i is given by (2.8), with V replaced by M_i^* . The values of h_i are given in Table II. From fits to pion photoproduction in the region of the $\Delta(1236)$,¹² the interaction radius d is found to be $1.2 \text{ F} = (160 \text{ MeV})^{-1}$. This value of d will be used for all four resonances.

The pion momentum is used in (2.7) to insure smooth behavior of the amplitude at the threshold, ω_T . The threshold behavior is $|(h/\omega)h^{2L}|$, and for large energies, $h \approx \omega$.

The constants C_i are obtained by calculating the unpolarized differential cross section in the center-of-mass system and fitting it to the Compton scattering data at constant c.m. angle. Using (2.1), the unpolarized cross section is given by

$$\begin{aligned}
 (d\sigma/d\Omega)_C = & (\alpha^2 M^2/V^2) \{ \frac{1}{2}(1+x^2)[|R_1|^2 + |R_2|^2] \\
 & + \frac{1}{2}(3-x^2)[|R_3|^2 + |R_4|^2] \\
 & + (1+3x^2)[|R_5|^2 + |R_6|^2] \\
 & + 2(1+x^2) \text{Re}(R_4 R_5^* + R_3 R_6^*) \\
 & + 2x \text{Re}(R_1 R_2^* + R_3 R_4^* + 2R_3 R_5^* + 2R_4 R_6^*) \\
 & + 2x(3+x^2) \text{Re}(R_5 R_6^*) \}. \quad (2.9)
 \end{aligned}$$

The Compton scattering data¹ are shown in Fig. 2(a) ($\theta^* = 90^\circ$) and 2(b) ($\theta^* = 65^\circ$) along with a fit to the data labeled set *a* in Table III. The fit in the region 400

$< \omega^{\text{lab}} < 550$ MeV is slightly improved in Fig. 2(a) when C_2 is increased. However, because of the large width of the $N(1400)$, there is substantial interference with the higher-mass resonances, causing larger values of C_2 to decrease the quality of the fit at higher energies.

The remaining three sets of couplings in Table III represent a decreasing amount of $N(1400)$ in the Compton amplitude. The fits obtained with these sets agree, within the errors, with the data in Fig. 2, except in the region $400 < \omega^{\text{lab}} < 550$ MeV.

Writing the scattering amplitude in (2.1) as

$$T_C = e_i' T_{ij} e_j,$$

then the optical theorem gives

$$-\frac{2\pi\alpha}{\omega} \left(\delta_{ij} - \frac{k_i k_j}{\omega^2} \right) \text{Im} T_{ij} = \sigma_{\text{tot}}, \quad (2.10)$$

where σ_{tot} is the total photon-proton cross section. The left-hand side of (2.10) is obtained from (2.1), (2.5), and (2.6) and shown in Fig. 3 for the four sets of constants in Table III. Also shown in Fig. 3 are the experimental determination of the quantity $\sigma^{\text{tot}}(\gamma p \rightarrow p\pi^0 + n\pi^+ + p\eta + p\pi^+\pi^-)$ ¹⁴ (dashed line) and three points from an experimental determination of the total photon-proton hadronic cross section.¹⁵ The fits in Table III are seen to agree well with the optical-theorem result (2.10).

In order to perform another test of the phenomenological cross section obtained from (2.9), we compare angular distributions with the available data at $\omega^{\text{lab}} = 210, 245, \text{ and } 310$ MeV.² The comparison using set *a* is shown in Fig. 4, where the phenomenological expression is seen to follow the data quite well.

III. PROTON COMPTON SCATTERING OF POLARIZED PHOTONS

We now proceed to calculate the proton Compton scattering cross sections for polarized incident photons. The differential cross sections for incoming photons polarized parallel and normal to the reaction plane will be denoted by $d\sigma_{\parallel}/d\Omega$ and $d\sigma_{\perp}/d\Omega$, respectively. The incident polarization vector in (2.1) for parallel polarization is given by

$$\mathbf{e}_{\parallel} = \frac{\mathbf{k}' - x\mathbf{k}}{(1-x^2)^{1/2}} \quad (3.1)$$

and for normal polarization by

$$\mathbf{e}_{\perp} = \frac{\mathbf{k} \times \mathbf{k}'}{(1-x^2)^{1/2}}. \quad (3.2)$$

¹⁴ E. Lohrmann, Review Talk given at the Lund International Conference on Elementary Particles, 1969 (unpublished).

¹⁵ H. G. Hilpert *et al.*, Phys. Letters **27B**, 474 (1968).

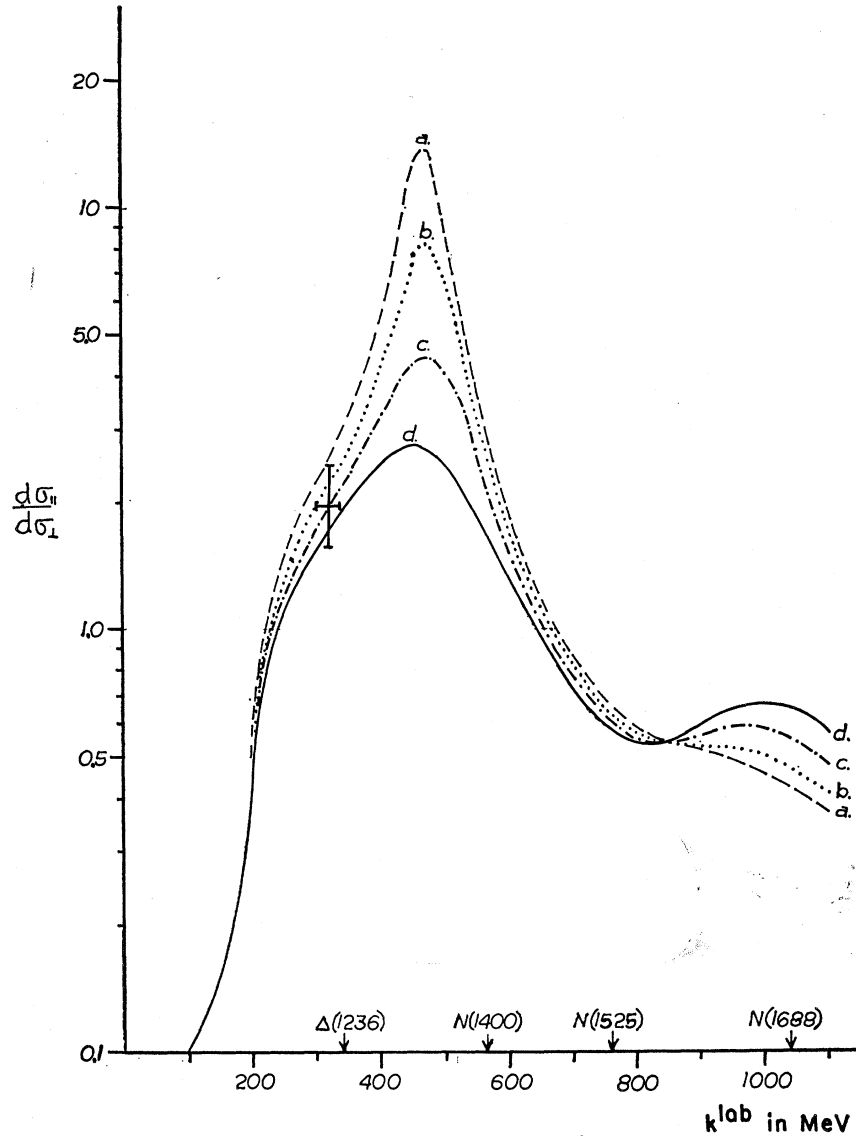


FIG. 5. Polarized-photon cross-section ratio, $\theta^*=90^\circ$. The letters correspond to the sets of constants in Table III. The experimental point is from Ref. 3.

Using (3.1) and (3.2) in (2.1), we obtain the following results:

$$\begin{aligned}
 d\sigma_{11}/d\Omega = & (\alpha^2 M^2/V^2) \{ x^2 |R_1|^2 + |R_2|^2 \\
 & + (2-x^2) |R_3|^2 + |R_4|^2 \\
 & + (1+3x^2) [|R_5|^2 + |R_6|^2] \\
 & + 2(1+x^2) \operatorname{Re}(R_4^* R_5 + R_3^* R_6) \\
 & + 2x \operatorname{Re}(R_1^* R_2 + R_3^* R_4 + 2R_3^* R_5 + 2R_4^* R_6) \\
 & + 2x(3+x^2) \operatorname{Re}(R_5^* R_6) \}, \quad (3.3)
 \end{aligned}$$

$$d\sigma_1/d\Omega = d\sigma_{11}/d\Omega \quad (\text{with } R_1 \leftrightarrow R_2, R_3 \leftrightarrow R_4, R_5 \leftrightarrow R_6).$$

The scalar functions obtained in Sec. II are used in (3.3) to obtain $d\sigma_{11}/d\sigma_1$. The results are shown in Fig. 5 for $\theta^*=90^\circ$. The four curves correspond to the four sets of constants C_i in Table III. Also shown in Fig. 5 is the experimental point of Barbiellini *et al.*,³ obtained in the

region of the $\Delta(1236)$, i.e.,

$$d\sigma_{11}/d\sigma_1 = 2.1_{-0.4}^{+0.5}.$$

We note in passing that if only magnetic dipole amplitudes are present, using (2.5) in (3.3), one obtains

$$\frac{d\sigma_{11}}{d\sigma_1} = \frac{5}{2+3x^2}$$

or a value of $d\sigma_{11}/d\sigma_1 = 2.5$ at $\theta^*=90^\circ$.

The most striking feature of Fig. 5 is the variation obtained in $d\sigma_{11}/d\sigma_1$ as one varies the amount of $N(1400)$ resonance contribution in the Compton amplitude. As one goes from set *a*, in which there is a maximal amount of $N(1400)$, to set *d*, in which there is no $N(1400)$ present, there is a variation of about a factor of 6 in the

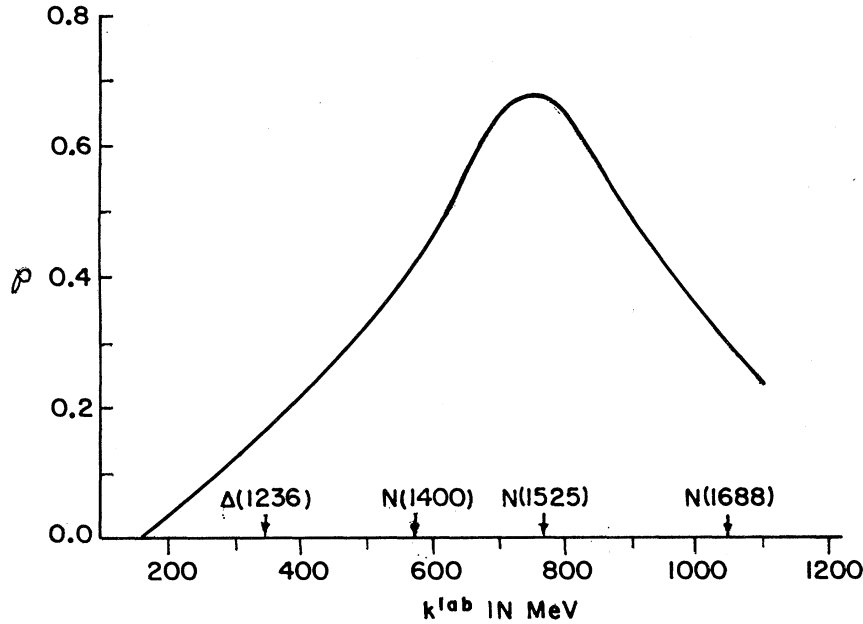


FIG. 6. Recoil-proton polarization, $\theta^* = 90^\circ$ (set *a*).

energy region between the $\Delta(1236)$ and $N(1400)$. This behavior of $d\sigma_{11}/d\sigma_{\perp}$ in this region is due to the fact that both the $\Delta(1236)$ and $N(1400)$ occur primarily in magnetic dipole amplitudes. As can be seen in (2.5), their contribution to the scalar function R_4 is opposite in sign, causing a cancellation to occur in $d\sigma_{\perp}/d\Omega$ in the energy region between the two resonances (R_2 does not contribute to $d\sigma_{\perp}/d\Omega$ at $\theta^* = 90^\circ$), leading to an enhancement of $d\sigma_{11}/d\sigma_{\perp}$.

IV. RECOIL-PROTON POLARIZATION

We next turn to recoil-proton polarization in Compton scattering. We calculate the polarization in the transverse plane, defined by

$$\mathcal{P} = \frac{d\sigma^{\uparrow} - d\sigma^{\downarrow}}{d\sigma^{\uparrow} + d\sigma^{\downarrow}}, \quad (4.1)$$

$$\mathcal{P} = \frac{(\alpha^2 M^2 / V^2)(1-x^2)^{1/2} \text{Im}[(R_2^* + xR_1^*)R_3 + (R_1^* + xR_2^*)R_4]}{(d\sigma/d\Omega)_c}. \quad (4.3)$$

Using the couplings in set *a*, the recoil-proton polarization is shown in Fig. 6 for $\theta^* = 90^\circ$. The maximum occurs in the region of the $N(1525)$. When the other sets of couplings in Table III are used, the polarization varies from the results in Fig. 6 by less than 10%.

V. DISCUSSION

The amplitude used in the above calculations has a number of deficiencies. Although the Born terms and π^0 and η^0 pole terms are treated correctly, the main features of polarized-photon scattering and recoil-

where \uparrow (\downarrow) indicates the scattering cross section with the final proton polarization along (opposite) the direction of the vector

$$\mathbf{n} = \frac{\mathbf{k} \times \mathbf{k}'}{(1-x^2)^{1/2}}.$$

The amplitude (2.1) is used along with the proton spinor projection operators

$$P_{\pm} = \frac{1}{2}(1 \pm \boldsymbol{\sigma} \cdot \mathbf{n}).$$

We first note that

$$\frac{d\sigma^{\uparrow}}{d\Omega} + \frac{d\sigma^{\downarrow}}{d\Omega} = \left(\frac{d\sigma}{d\Omega} \right)_c \quad (4.2)$$

given in (2.9). It is a straightforward calculation to obtain $d\sigma^{\uparrow} - d\sigma^{\downarrow}$, with the result

proton polarization are due to the nucleon resonance contributions. In the energy region of interest, the $N(1550)$ and $\Delta(1640)$ *s*-wave resonances have been ignored since their elasticities into the π -*N* channel are only 30%. Furthermore, only the dominant multipole amplitudes are used for the nucleon resonances that are retained. The point of view taken is that in the unitarity sum in a dispersion approach, the π -*N* intermediate states dominate, even up to incident laboratory photon energies of 1 GeV. The hope is that the presence of other intermediate states, especially at the higher energies, is

compensated for by the fact that the resonance couplings are purely phenomenological, i.e., obtained by a fit to the differential cross-section data at fixed center-of-mass angles.

The strong dependence of the ratio $d\sigma_{11}/d\sigma_1$ on the amount of $N(1400)$ resonance contribution to the Compton amplitude, as illustrated in Fig. 5, is expected to be only weakly affected by the above considerations. The variation in $d\sigma_{11}/d\sigma_1$ occurs in an energy region below the $N(1550)$ and $\Delta(1640)$ resonances where they

would have had little effect if they had been included, due to the threshold behavior of the energy-dependent widths. Furthermore, intermediate states other than the $\pi-N$ states are expected to make only a small contribution to the Compton amplitude in this energy region. We conclude that a measurement of the scattering of polarized photons at incident laboratory energies between 450 and 500 MeV should give a qualitative determination of the amount of P_{11} resonance in the proton Compton scattering amplitude.

Vector-Meson and Dipion Production in Lepton-Nucleon Collisions*

A. PAIS

Rockefeller University, New York, New York 10021

(Received 12 November 1969)

The electroproduction of ρ , ω , and ϕ mesons is discussed. The spin-density matrix elements are shown to satisfy a number of conditions if and where the production is dominated by Pomanchuk exchange. Constraints are also given for the case that a single spin-parity (of type $0^\pm, 1^\pm$) dominates the t channel in some kinematic region. The extension to the production of a 2π continuum is straightforward. Vector-meson and 2π production by neutrinos is also treated.

I. INTRODUCTION

THE quantum numbers of the ρ , ω , and ϕ mesons are such that their high-energy electroproduction can be dominated by the Pomanchuk mechanism (in contrast to single-pion production¹). The experimental study of these processes is therefore of considerable interest, as it will afford a first opportunity to find out whether the notion of Pomanchuk dominance applies to specific reaction initiated by virtual massive photons, just as pion production is the simplest instance, in this context, where neutrino reactions are concerned.²

Pomanchuk dominance entails three qualitative aspects: (1) a power-law behavior in the final-state hadronic energy variable (for what follows it is not decisive whether this behavior is exact or approximate); (2) t -channel dominance by a natural-parity sequence; (3) all participating amplitudes have a common phase dictated by the signature factor. These various aspects will prove to reflect themselves in the structure of the spin-density matrix elements for $\rho \rightarrow 2\pi$, $\omega \rightarrow 3\pi$, $\phi \rightarrow K\bar{K}$ (Sec. III B). The arguments can be extended in several ways.

(1) They can be made to apply to the high-energy behavior of 2π production over a considerable range of the invariant mass of the 2π system. Since this permits

sizable integrations over that mass variable, $e+p \rightarrow e+p+2\pi$ is actually the simplest experimental process from the present point of view (Sec. III D).

(2) For either vector-meson or 2π production, electroproduction processes turn out to be rich in implications for t -channel dominance by a fixed spin-parity mechanism. This may include several distinct possibilities (depending on the kinematic region of interest) such as peripheral production dominated by a single particle, or also the influence of fixed singularities³ whose physical meaning is less clear and whose influence may perhaps extend beyond the diffractive region (Sec. III C).

(3) All these questions may likewise be raised for the corresponding neutrino reactions.

These various topics are the subject of the present paper. The hadronic aspects of the mentioned reactions can all be symbolized by (V =vector meson)

$$\text{current}+p \rightarrow p+V, \quad (1.1)$$

$$\text{current}+p \rightarrow p+\pi+\pi. \quad (1.2)$$

It is helpful to start with a few general remarks on Eq. (1.2), from which it will be seen that the discussion of Eq. (1.1) in many ways emerges as a special case.

The reaction (1.2) is characterized by eight variables (apart from spin). It will be shown that the differential cross section consists of a sum of terms each of which

* Work supported in part by the U. S. Air Force Office of Scientific Research under Grant No. AF-AFOSR-69-1629.

¹ See also H. Harari, Phys. Rev. Letters **24**, 286 (1970).

² A. Pais and S. B. Treiman, Phys. Rev. (to be published). This paper is cited hereafter as I.

³ For a recent survey of these questions see G. C. Fox and D. Z. Freedman, Phys. Rev. **182**, 1628 (1969). This paper contains detailed references to earlier work on this problem.